Report

Current Biology

Purging of Strongly Deleterious Mutations Explains Long-Term Persistence and Absence of Inbreeding Depression in Island Foxes

Highlights

- Island fox genomes have low diversity and an elevated load of deleterious mutations
- Congenital defects common in inbred carnivores are rare in island fox skeletons
- Simulations suggest that island foxes have purged strongly deleterious recessive alleles
- Purging may have enabled long-term persistence and rapid recovery from bottlenecks

Authors

Jacqueline A. Robinson, Caitlin Brown, Bernard Y. Kim, Kirk E. Lohmueller, Robert K. Wayne

Correspondence

jacqueline.robinson@ucsf.edu

In Brief

Robinson et al. analyze genomic, morphological, and simulated data to understand why island foxes do not suffer from inbreeding depression and rapidly rebounded from recent bottlenecks, despite having low genomic diversity and an elevated number of deleterious alleles. They suggest purging of recessive deleterious alleles as a possible mechanism.

Robinson et al., 2018, Current Biology *28*, 3487–3494
November 5, 2018
https://doi.org/10.1016/j.cub.2018.08.066

CellPress

Current Biology
Report

Purging of Strongly Deleterious Mutations Explains Long-Term Persistence and Absence of Inbreeding Depression in Island Foxes

Jacqueline A. Robinson,[1,4,6,*] Caitlin Brown,[1] Bernard Y. Kim,[1] Kirk E. Lohmueller,[1,2,3,5] and Robert K. Wayne[1,5]
[1]Department of Ecology and Evolutionary Biology, University of California, Los Angeles, Los Angeles, CA 90095, USA
[2]Interdepartmental Program in Bioinformatics, University of California, Los Angeles, Los Angeles, CA 90095, USA
[3]Department of Human Genetics, David Geffen School of Medicine, University of California, Los Angeles, Los Angeles, CA 90095, USA
[4]Present address: Institute for Human Genetics, University of California, San Francisco, San Francisco, CA 94143, USA
[5]These authors contributed equally
[6]Lead Contact
*Correspondence: jacqueline.robinson@ucsf.edu
https://doi.org/10.1016/j.cub.2018.08.066

SUMMARY

The recovery and persistence of rare and endangered species are often threatened by genetic factors, such as the accumulation of deleterious mutations, loss of adaptive potential, and inbreeding depression [1]. Island foxes (*Urocyon littoralis*), the dwarfed descendants of mainland gray foxes (*Urocyon cinereoargenteus*), have inhabited California's Channel Islands for >9,000 years [2–4]. Previous genomic analyses revealed that island foxes have exceptionally low levels of diversity and elevated levels of putatively deleterious variation [5]. Nonetheless, all six populations have persisted for thousands of generations, and several populations rebounded rapidly after recent severe bottlenecks [6, 7]. Here, we combine morphological and genomic data with population-genetic simulations to determine the mechanism underlying the enigmatic persistence of these foxes. First, through analysis of genomes from 1929 to 2009, we show that island foxes have remained at small population sizes with low diversity for many generations. Second, we present morphological data indicating an absence of inbreeding depression in island foxes, confirming that they are not afflicted with congenital defects common to other small and inbred populations. Lastly, our population-genetic simulations suggest that long-term small population size results in a reduced burden of strongly deleterious recessive alleles, providing a mechanism for the absence of inbreeding depression in island foxes. Importantly, the island fox illustrates a scenario in which genetic restoration through human-assisted gene flow could be a counterproductive or even harmful conservation strategy. Our study sheds light on the puzzle of island fox persistence, a unique success story that provides a model for the preservation of small populations.

RESULTS

Minimal Impact of Recent Demography on Island Fox Genomes

Previous analysis of whole genome sequences from island foxes sampled in 1988 revealed dramatically reduced levels of diversity and increased levels of putatively deleterious alleles relative to the mainland gray fox [5]. On the smallest island, San Nicolas, the population is nearly monomorphic across its entire genome [5]. Beginning in the 1990s, four populations declined >90% due to novel predators (San Miguel, Santa Rosa, and Santa Cruz) and disease (Santa Catalina) but subsequently rebounded under human management in the fastest recovery of any mammal under the Endangered Species Act to date [6, 7]. We sequenced whole genomes of foxes sampled in 2000–2009 from each island to determine whether recent extreme bottlenecks reduced variation or whether very low genetic variation is a persistent feature of island fox genomes. Additionally, we sequenced DNA isolated from bone fragments from a 1929 San Nicolas island fox and DNA from a Northern California gray fox. Combined with existing sequences, our dataset includes 16 genomes with 13×–23× coverage (Table S1). All sequences were aligned to the domestic dog (*Canis familiaris*) reference genome canFam3.1. Phylogenetic analyses show that island fox genomes cluster by population and that southern and northern island populations define distinct clusters, consistent with prior studies (Figures 1A, 1B, and S1) [4, 5, 8, 9].

Overall, we did not find significant changes in genome-wide heterozygosity between island foxes sampled from the same population at different times (Figure 1B). Among populations that bottlenecked in the 1990s, two genomes showed slightly higher heterozygosity after 2000 than in 1988 (Santa Catalina and Santa Cruz), whereas two showed slightly lower heterozygosity (San Miguel and Santa Rosa). Similarly, in San Nicolas and San Clemente, genome-wide heterozygosity was essentially unchanged from 1988 to after 2000. These minor differences between genomes over time are not statistically significant (Wilcoxon signed-rank test, $p = 1$) and may be expected due to small inter-individual differences in heterozygosity. Robinson et al. [5] hypothesized that the genomic flatlining of San Nicolas foxes may have resulted, in part, from a suspected bottleneck in the

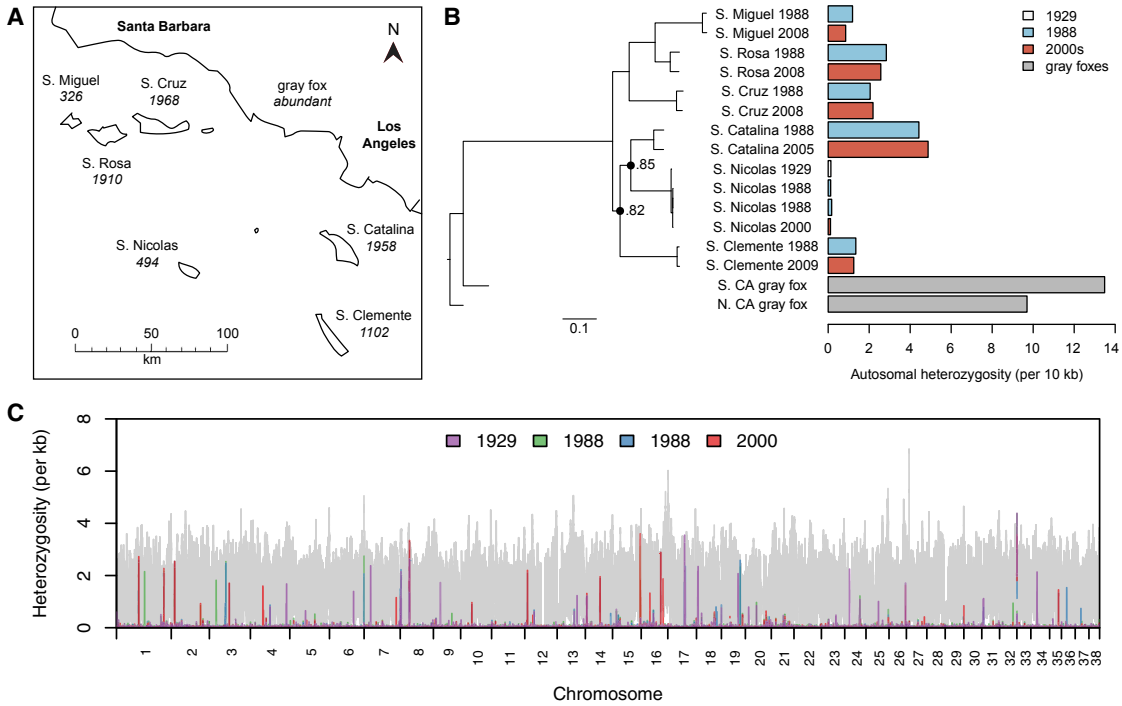

Figure 1. Genetic Relationships and Heterozygosity of Island Fox Genomes

(A) Map of the Channel Islands with estimated island fox census sizes [8].

(B) Left: maximum-likelihood tree based on >12,000 SNPs. Nodes have 100% bootstrap support, except where noted. Right: mean per-site heterozygosity across the autosomal genome. See also Figure S1 and Table S1.

(C) Heterozygosity in 100 kb windows with a 10 kb step size across the autosomal genome shows the genomic flatlining punctuated by occasional peaks of heterozygosity in San Nicolas foxes. Heterozygosity in the Southern California gray fox is shown in gray. The x axis coordinates correspond to the reference dog genome. See also Tables S2 and S3.

1970s [10]. However, the 1929 genome bears exceptionally low diversity (1.33×10^{-5} heterozygotes/base pair), similar to genomes from 1988 and 2000 (mean = 1.35×10^{-5} heterozygotes/base pair) (Figures 1B and 1C). The genomic flatlining of San Nicolas foxes is therefore an enduring characteristic of this population, underscoring the mystery concerning its long-term persistence.

Previous analysis of remnant peaks of heterozygosity in San Nicolas genomes revealed strong enrichment for olfactory function [5]. We revisited the question of whether patterns of heterozygosity in San Nicolas foxes are consistent with neutral evolution or the result of selection maintaining diversity at functionally important loci. Among peaks of heterozygosity from all four San Nicolas genomes, only 43.9% were present in two or more individuals. The 1929 genome was the most divergent, with only 41.5% of its peaks shared with at least one other individual, suggesting that peaks of heterozygosity are not strongly conserved over time. We conducted coalescent simulations [11] under plausible models of San Nicolas demographic history [5] to determine whether variation in the sequenced genomes is predicted by these neutral demographic models. We found that the empirical numbers of peaks, average peak widths, and proportions of shared peaks all fell within the middle 95% of values obtained through simulation (Table S2), suggesting that demographic processes alone can account for empirical patterns of variation in peaks of heterozygosity within and between San Nicolas fox genomes.

Despite the lack of evidence that peaks of heterozygosity are constrained by selection, peaks in the 1929 and 2000 San Nicolas genomes are strongly enriched for olfactory receptor (OR) genes ($p \leq 3.57 \times 10^{-16}$), as they are in the genomes from 1988 ($p \leq 2.78 \times 10^{-15}$) (Table S3, KEGG: 04740). Strikingly, 39.3%–50.7% of peaks in San Nicolas genomes overlap OR genes. However, these peaks vary between individuals; 37.2% of peaks containing OR genes are found in only one San Nicolas genome, despite consistency in coverage and peak thresholds ($1.67–1.72 \times 10^{-4}$ heterozygotes/base pair) across all four individuals. Peaks of heterozygosity in mainland gray fox genomes are also enriched for OR genes ($p \leq 4.98 \times 10^{-3}$). Enrichment of OR genes in gray fox peaks is unsurprising, since OR genes are highly variable in mammals generally, suggesting that they have an elevated rate of evolution [12]. Given high initial variation, OR genes may be among the last to lose diversity as drift erodes heterozygosity in island genomes over time. Alternatively, high variation in OR gene regions may be due to alignment errors, since OR gene repertoires evolve rapidly through gene duplication, pseudogenization, and loss [12]. Nonetheless, even if peaks of heterozygosity containing OR genes result from read misalignment, the fact that peaks are not consistently observed across San Nicolas foxes implies that some variability, either copy-number variation or true heterozygosity, persists in these regions.

We found that levels of non-neutral variation are largely similar between island fox genomes sampled at different times.

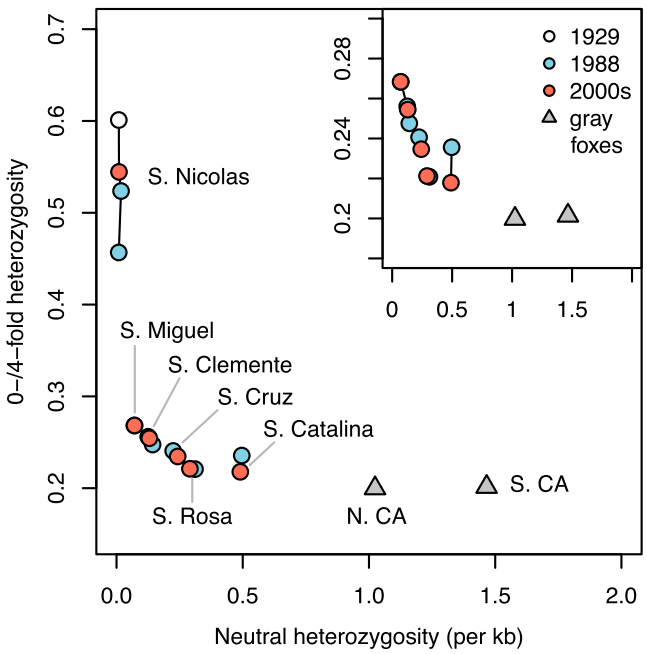

Figure 2. Island Fox Genomes Contain High Proportions of Amino Acid-Changing Mutations and Low Neutral Diversity

A negative relationship exists between neutral genetic diversity (proxy for effective population size) and the ratio of heterozygosity at zero-fold relative to four-fold degenerate sites (proxy for efficacy of selection). Solid black lines connect individuals from the same population. The relationship holds even when removing San Nicolas (inset). See also Figure S2 and Table S4.

Comparison of heterozygosity at zero-fold and four-fold degenerate sites within protein-coding regions (i.e., sites where all or none of the possible nucleotide changes alter the encoded amino acid, respectively) showed that island fox genomes have a high ratio of amino-acid-changing to non-amino-acid-changing variants relative to gray foxes (Figure 2). We calculated heterozygosity within a set of putatively neutral loci across the genome as a proxy for effective population size. Together, the elevated proportions of putatively damaging mutations at zero-fold degenerate sites and the reduction in neutral heterozygosity demonstrate the genomic consequences of enhanced drift relative to selection on the islands. Neutral diversity and ratios of zero-fold to four-fold heterozygosity were essentially unchanged between genomes from 1988 and after 2000. All San Nicolas genomes showed a strongly elevated ratio of heterozygosity at zero-fold relative to four-fold degenerate sites, although the small number of heterozygous sites produces high variance of this statistic [5].

We further examined predicted loss-of-function (LOF) and putatively deleterious missense mutations (Figure S2; Table S4). Across all populations, island foxes had elevated homozygosity of derived alleles, with more than double the number of homozygous LOF and deleterious missense alleles compared to gray foxes ($p < 1.75 \times 10^{-10}$). Further, island genomes contained an excess total number of putatively deleterious alleles per genome. Relative to gray foxes, island foxes from 1988 had 2.3% more deleterious missense alleles ($p = 1.11 \times 10^{-10}$) and 4.9% more LOF alleles ($p = 2.43 \times 10^{-3}$) per genome, and island foxes from after 2000 contained 1.7% more deleterious missense alleles ($p = 4.68 \times 10^{-9}$) and 3.3% more LOF alleles per genome ($p = 0.0560$). Thus, regardless of whether deleterious mutations are additive or recessive, island foxes are predicted to have reduced fitness compared to gray foxes due to elevated homozygosity and an increased total number of deleterious alleles.

Congenital Skeletal Defects Are Rare in Island and Gray Foxes

Previous studies of inbred carnivoran skeletons have found a suite of pathologies linked to low genetic diversity, particularly in the skull and vertebral column [13–15]. For example, a study of gray wolves (*Canis lupus*) on Isle Royale, Michigan, found that 58% of individuals exhibited vertebral anomalies within ten generations of the population's founding due to extreme inbreeding [15]. We inspected skulls (n = 141) and complete skeletons (n = 163) of adult foxes sampled in 1929–2013 from all six islands and the mainland to identify anomalies that could indicate inbreeding depression. Congenital deformities were present but rare in island foxes; among 119 specimens, only seven possessed developmental pathologies. Observed congenital defects included extra lumbar vertebrae (n = 1), lumbosacral transitional vertebrae (LSTVs; n = 1), sacrocaudal transitional vertebrae (SCTVs; n = 3), and malocclusion teeth (n = 2) (Figure 3A; Table S5). Among 43 San Nicolas specimens, only one congenital defect (malocclusion incisors) was observed. In contrast, traumatic pathologies indicating prior injuries, primarily from suspected vehicular collisions, were common in island foxes, as evidenced by specimens with bone fractures and indications of infection (Figure 3B; Table S5). Unlike the rare congenital malformations that we observed, vehicular impacts most likely compromise mobility and contribute to early mortality.

We note that although island foxes have low levels of congenital skeletal defects, this finding does not preclude the presence of soft tissue traits commonly associated with inbreeding, such as syndactyly and reproductive anomalies [16, 17]. Further study is needed to rule out the presence of such traits in island foxes, but they have not been previously reported despite over a decade of intensive management, including several years of captive breeding [6], ejaculate quality assays [18], and necropsy of road-killed individuals [19].

Among 44 gray fox specimens, few pathologies were observed. Congenital defects in gray foxes included LSTV (n = 1), SCTV (n = 1), and achondroplastic dwarfism (n = 1). In contrast to island foxes, traumatic pathologies were uncommon in gray foxes. Healed fractures consistent with vehicular impacts were not observed, though we note that this may be due to ascertainment bias if road killed mainland foxes were less likely to be included in museum collections.

Using Fisher's exact test, we determined that there was no significant difference ($p = 0.663$) in the proportion of congenital defects between island foxes and mainland gray foxes (Figure 3A). However, there was a significant difference between the islands in the proportion of probable collision injuries ($p = 3.90 \times 10^{-3}$) (Figure 3B). We calculated relative risk scores and performed a permutation test to assess significant differences in collision injuries between populations (Table S5). We found that foxes on the three islands with paved roads and

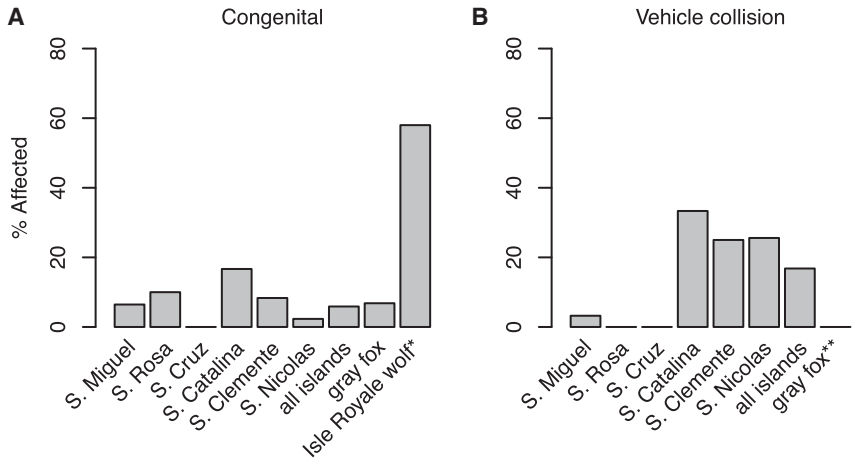

Figure 3. Prevalence of Skeletal Pathologies in Island and Gray Foxes

(A) Incidence of congenital defects in gray and island foxes (this study) compared to Isle Royale wolves (*) [15].

(B) Incidence of traffic-related pathologies in gray and island foxes. The absence of traffic-related pathologies in gray foxes (**) is possibly due to ascertainment bias against the retrieval of mainland fox roadkill.

Sample sizes are as follows: S. Miguel, n = 31; S. Rosa, n = 10; S. Cruz, n = 5; S. Catalina, n = 6; S. Clemente, n = 24; S. Nicolas, n = 43; all islands, n = 119; gray foxes, n = 44; Isle Royale wolves, n = 36. See also Table S5.

substantial human habitation (Santa Catalina) or naval bases (San Clemente and San Nicolas) face significantly higher risks of vehicle collisions. No probable collisions were recorded in the Santa Cruz, Santa Rosa or gray fox samples. Overall, our morphological assessment supports the hypothesis that island foxes do not exhibit canonical signs of inbreeding depression, though some populations are adversely affected by vehicular traffic.

Predicted Genetic Variation in Large Mainland versus Small Island Populations

We hypothesized that the absence of inbreeding depression in island foxes may be attributed to purging of strongly deleterious recessive mutations in island populations relative to the mainland, despite the overall accumulation of deleterious variants observed in island genomes. To test this hypothesis, we conducted forward-in-time simulations [20] under a range of demographic models (Figure 4A), each consisting of a mainland population of 10,000 diploids giving rise to an island population with a final size of 1,000 diploids. After 10,000 generations, we counted the number of strongly deleterious ($s < -0.01$; Figure 4B), moderately deleterious ($-0.01 \leq s < -0.001$; Figure 4C), weakly deleterious ($-0.001 \leq s < 0$; Figure 4D), and neutral ($s = 0$; Figure 4E) mutations per individual. To explore the impact of dominance, we performed one set of simulations with recessive mutations ($h = 0$) and one set of simulations with additive mutations ($h = 0.5$).

Results were strikingly consistent across all six demographic scenarios, indicating that the predominant factor driving levels of variation is long-term small population size on the islands, rather than transient effects. Except in the case of strongly deleterious mutations, homozygosity was always higher in island genomes relative to mainland genomes ($p < 10^{-7}$). The total number of deleterious alleles per individual on the islands relative to the mainland varied according to selection and dominance coefficients (Figures 4B–4E). In simulations in which mutations were additive, island genomes contained, on average, 9.97% more deleterious alleles per individual overall ($p \leq 3.09 \times 10^{-5}$), primarily due to the accumulation of weakly and moderately deleterious alleles. However, numbers of strongly deleterious additive alleles were equivalent between the islands and the mainland, which is expected since these mutations sharply reduce fitness in both homozygotes and heterozygotes and are thus readily removed by selection in small and large populations.

In contrast, rare recessive mutations are exposed to selection more frequently in small populations due to elevated homozygosity and are therefore removed more efficiently than in larger populations. Although the total number of recessive deleterious alleles was not significantly different between individuals from the islands and the mainland, moderately and strongly deleterious recessive alleles were greatly depleted. Island genomes contained, on average, 37.1% fewer moderately deleterious recessive alleles ($p < 10^{-7}$) and 67.7% fewer strongly deleterious recessive alleles ($p < 10^{-7}$) compared to the mainland. Furthermore, there were no simulations in which the average number of strongly deleterious recessive alleles was higher in island genomes compared to the mainland (Figure 4B).

We also performed simulations under a range of smaller island population sizes (N = 500, 200, 100, and 50) to determine whether purging of strongly deleterious mutations still occurred. We expected that population size would modulate selection against deleterious alleles, as predicted by the nearly neutral theory, whereby mutations with $|s| < 1/2N$ behave as if they are neutral despite their effects on fitness [21]. Overall, we found that purging of recessive deleterious alleles became weaker and the accumulation of additive deleterious alleles became more severe as population size declined (Table S6). However, exceptionally deleterious recessive alleles ($s < -0.1$) were always depleted in the smaller island populations ($p < 10^{-7}$). In sum, these findings suggest that individuals derived from historically small populations carry a reduced burden of strongly deleterious recessive alleles relative to individuals from a large outbred population, reducing the former's risk of inbreeding depression.

DISCUSSION

Our genomic analyses show that recent catastrophic bottlenecks had limited impact on island fox genomes, indicating that exceptionally low heterozygosity and higher levels of putatively deleterious alleles are caused by historically small population size. We confirm the apparent lack of inbreeding depression

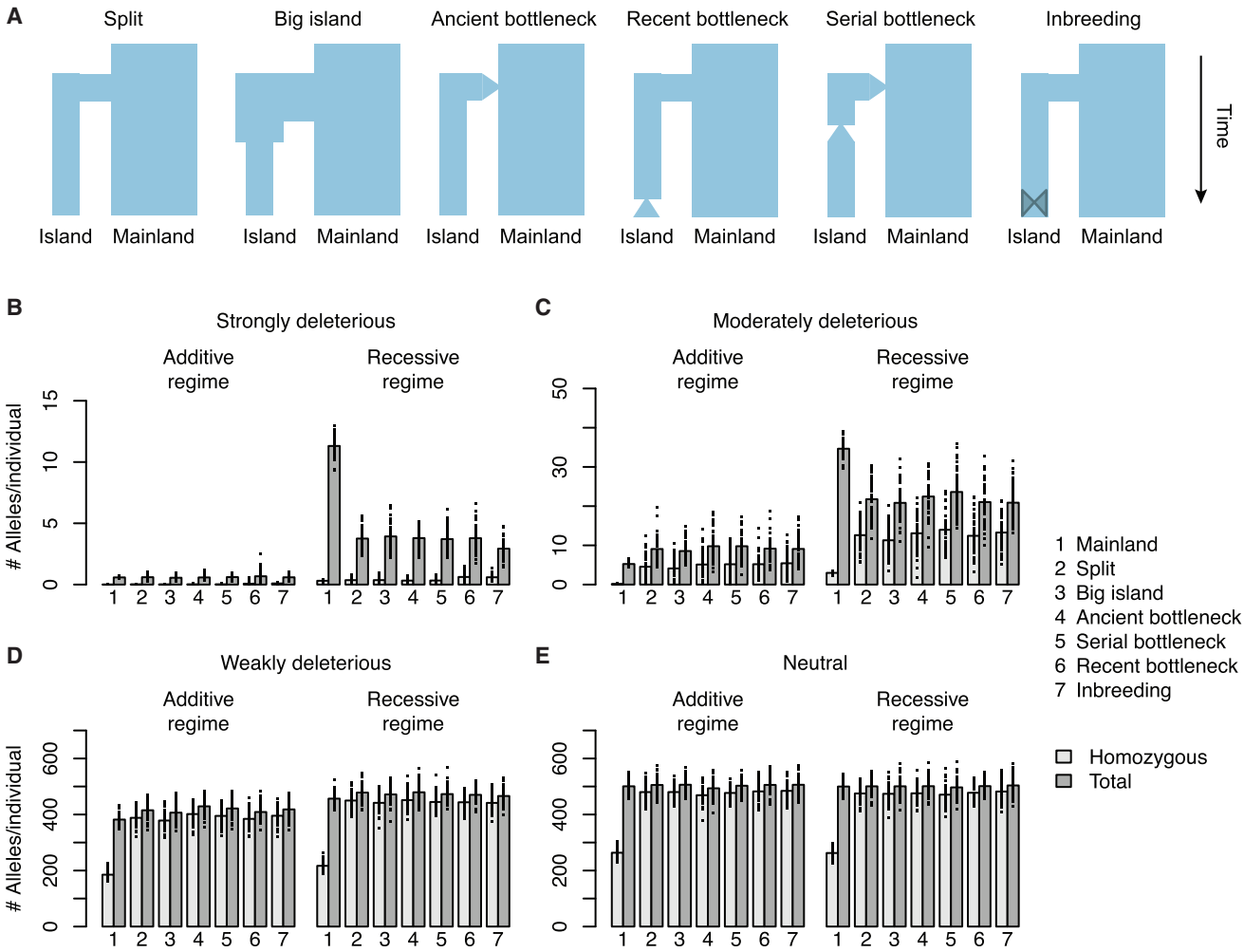

Figure 4. The Number of Strongly Deleterious Recessive Alleles per Individual Is Reduced in Island Populations

(A) Depictions of demographic models used in simulations (not to scale). At the end of the simulations, $N_{mainland}$ = 10,000 diploids, N_{island} = 1,000 diploids. (B–E) Charts showing the total number of derived alleles and the number of homozygous derived alleles per individual by dominance and selection strength. Dots represent the mean per individual within a single replicate; bar height represents the mean across all 50 replicates. Selection strengths are as follows: (B) strongly deleterious, $-1 \leq s < -0.01$; (C) moderately deleterious, $-0.01 \leq s < -0.001$; (D) weakly deleterious, $-0.001 \leq s < 0$; and (E) neutral, $s = 0$. Simulations include a mixture of neutral and deleterious alleles in which deleterious alleles are either entirely additive (additive regime) or entirely recessive (recessive regime). See also Table S6.

in island foxes through detailed morphological assessment and, through demographic simulations, demonstrate that this lack of inbreeding depression may be explained by purging of strongly deleterious alleles in persistently small populations. Potentially, the purging of strongly deleterious alleles in island foxes may have enabled their long-term persistence, as well as rapid recovery from recent severe bottlenecks.

Sluggish recovery from bottlenecks is a characteristic of severely inbred populations [16, 22]. For example, the wolf population of Isle Royale National Park, founded less than a hundred years ago, is intensely inbred with evidence of inbreeding depression (Figure 1), has not increased in size despite an abundance of prey, and is destined for extinction [15, 23]. Large outbred populations, such as the mainland source population for Isle Royale wolves, most likely carry a greater hidden load of recessive deleterious mutations, increasing the risk of inbreeding depression after population decline. Experiments with houseflies (*Musca domestica*) have found that purging with population persistence is more likely when the rate of inbreeding is slow, as might occur in a chronically small population, rather than fast, as in a sudden extreme bottleneck [24]. A previous history of purging of strongly deleterious recessive variants due to long-term small population size most likely pre-adapted island foxes to rapid recovery from recent bottlenecks.

Few examples of intentional inbreeding to facilitate purging of strongly deleterious alleles are known [25], though purging as a result of long-term reduced population sizes may conceivably be a factor in other cases of persistence with low genome-wide diversity [26, 27]. In contrast, examples of inbreeding depression are frequent in both wild and captive environments, and minimizing inbreeding is commonly a paramount concern of captive management efforts [28, 29]. Under long-term small

population size, weakly deleterious mutations may accumulate, slightly beneficial mutations may be lost, and depletion of genetic variation could compromise adaptability [1]. Rapid recovery of island fox populations after recent bottlenecks suggests that weakly deleterious mutations have not seriously compromised their fitness, at least for several thousand generations, though the progressive fixation and accumulation of such mutations over time is predicted to ultimately lead to mutational meltdown and extinction [30]. Our results suggest that this process may take place gradually over thousands of generations, if it occurs at all before other non-genetic factors cause extinction.

One final consideration in the persistence of island foxes is that historically, island foxes may have benefitted from a relatively benign environment. Recently, however, island fox populations have been threatened by anthropogenic changes in their environment (e.g., traffic collisions, novel diseases, and predators) [6]. A recent decline in the San Nicolas population due to unknown causes has resurrected the idea that genetic rescue, or human-assisted migration, may be necessary to preserve island fox populations [3, 9]. If the recent decline is not the result of inbreeding depression, but is rather due to environmental stressors, genetic rescue may not materially enhance the likelihood of population persistence and would compromise the genetic distinction of the population. Genetic rescue should not be used as a conservation technique for historically small populations, as on many islands, without compelling evidence of inbreeding depression. A systematic survey to detect inbreeding depression (assays of sperm quality, reproductive success, survivorship, etc.) is necessary before considering genetic rescue as a conservation strategy for island foxes. We advocate for continued close monitoring of island fox populations, ''watchful waiting,'' as in slowly developing cancers, to ensure a swift response in the event of a catastrophic decline.

In conclusion, the small population paradigm emphasizing an ''extinction vortex,'' partly driven by genetic factors [31], may not be an appropriate model when purging of strongly deleterious alleles has occurred through historically small population size. Of course, the fate of many small populations may be extinction before purging can occur. However, the independent long-term persistence of all six island fox populations for thousands of years suggests that small populations on the order of a few hundred individuals can persist over evolutionary timescales and provides a model for the preservation of small fragmented populations.

STAR★METHODS

Detailed methods are provided in the online version of this paper and include the following:

- KEY RESOURCES TABLE
- CONTACT FOR REAGENT AND RESOURCE SHARING
- EXPERIMENTAL MODEL AND SUBJECT DETAILS
- METHOD DETAILS
- QUANTIFICATION AND STATISTICAL ANALYSIS
  - Analysis of variation in island and gray fox genomes
  - Coalescent simulations under San Nicolas demographic models
  - Morphological assay of gray and island fox museum specimens
  - Forward simulations of genetic variation in island versus mainland populations
- DATA AND SOFTWARE AVAILABILITY

SUPPLEMENTAL INFORMATION

Supplemental Information includes two figures and six tables and can be found with this article online at https://doi.org/10.1016/j.cub.2018.08.066.

ACKNOWLEDGMENTS

We thank the National Park Service, the Catalina Island Conservancy, Dennis Hedgecock, and William Andelt for sharing samples used for genomic sequencing. We thank Paul Collins for advice and access to specimens and the Los Angeles County Museum of Natural History, the Santa Barbara Museum of Natural History, and the Donald Ryder Dickey Bird and Mammal Collection at the University of California, Los Angeles, for the use of their collections. This work was supported with funding from University of California President's Catalyst Award CA-16-376437 to R.K.W. and NIH grant R35GM119856 to K.E.L. This work used the Vincent J. Coates Genomics Sequencing Laboratory at University of California, Berkeley, supported by NIH Instrumentation Grant S10 OD018174.

AUTHOR CONTRIBUTIONS

J.A.R. and R.K.W. conceived of and designed the research. C.B. conducted morphological analysis, J.A.R. conducted genomic analyses, and J.A.R. and B.Y.K. conducted simulations. All authors contributed to the interpretation of results. J.A.R. and C.B. wrote the paper, with input and approval from all authors. K.E.L. and R.K.W. jointly supervised this work.

DECLARATION OF INTERESTS

The authors declare no competing interests.

Received: March 3, 2018
Revised: July 3, 2018
Accepted: August 31, 2018
Published: October 25, 2018

REFERENCES

1. Frankham, R. (2005). Genetics and extinction. Biol. Conserv. *126*, 131–140.
2. Collins, P.W. (1991). Interaction between island foxes (*Urocyon littoralis*) and Indians on islands off the coast of Southern California: I. Morphologic and archaeological evidence of human assisted dispersal. J. Ethnobiol. *11*, 51–81.
3. Vellanoweth, R.L. (1998). Earliest island fox remains on the southern Channel Islands: evidence from San Nicolas Island, California. J. Calif. Gt. Basin Anthropol. *20*, 100–108.
4. Hofman, C.A., Rick, T.C., Hawkins, M.T., Funk, W.C., Ralls, K., Boser, C.L., Collins, P.W., Coonan, T., King, J.L., Morrison, S.A., et al. (2015). Mitochondrial genomes suggest rapid evolution of dwarf California Channel Islands foxes (*Urocyon littoralis*). PLoS ONE *10*, e0118240.
5. Robinson, J.A., Ortega-Del Vecchyo, D., Fan, Z., Kim, B.Y., vonHoldt, B.M., Marsden, C.D., Lohmueller, K.E., and Wayne, R.K. (2016). Genomic flatlining in the endangered island fox. Curr. Biol. *26*, 1183–1189.
6. Coonan, T.J., Schwemm, C.A., and Garcelon, D.K. (2010). Decline and Recovery of the Island Fox: A Case Study for Population Recovery (Cambridge University Press).
7. US Fish and Wildlife Service (2016). Removing the San Miguel Island fox, Santa Rosa Island fox, and Santa Cruz Island fox from the federal list of Endangered and Threatened wildlife, and reclassifying the Santa

Catalina Island fox from Endangered to Threatened; final rule. Fed. Regist. *81*, 53315–53333.

8. Wayne, R.K., George, S.B., Gilbert, D., Collins, P.W., Kovach, S.D., Girman, D., and Lehman, N. (1991). A morphologic and genetic study of the island fox, *Urocyon littoralis*. Evolution *45*, 1849–1868.
9. Funk, W.C., Lovich, R.E., Hohenlohe, P.A., Hofman, C.A., Morrison, S.A., Sillett, T.S., Ghalambor, C.K., Maldonado, J.E., Rick, T.C., Day, M.D., et al. (2016). Adaptive divergence despite strong genetic drift: genomic analysis of the evolutionary mechanisms causing genetic differentiation in the island fox (*Urocyon littoralis*). Mol. Ecol. *25*, 2176–2194.
10. Laughrin, L.L. (1980). Populations and status of the island fox. In The California Islands: Proceedings of a Multi-disciplinary Symposium, D.M. Power, ed. (Santa Barbara Museum of Natural History), pp. 745–749.
11. Kelleher, J., Etheridge, A.M., and McVean, G. (2016). Efficient coalescent simulation and genealogical analysis for large sample sizes. PLoS Comput. Biol. *12*, e1004842.
12. Niimura, Y., and Nei, M. (2007). Extensive gains and losses of olfactory receptor genes in mammalian evolution. PLoS ONE *2*, e708.
13. Marker, L.L., and Dickman, A.J. (2004). Dental anomalies and incidence of palatal erosion in Namibian cheetahs (*Acinonyx jubatus jubatus*). J. Mammal. *85*, 19–24.
14. Räikkönen, J., Bignert, A., Mortensen, P., and Fernholm, B. (2006). Congenital defects in a highly inbred wild wolf population (*Canis lupus*). Mamm. Biol. *71*, 65–73.
15. Räikkönen, J., Vucetich, J.A., Peterson, R.O., and Nelson, M.P. (2009). Congenital bone deformities and the inbred wolves (*Canis lupus*) of Isle Royale. Biol. Conserv. *142*, 1025–1031.
16. Roelke, M.E., Martenson, J.S., and O'Brien, S.J. (1993). The consequences of demographic reduction and genetic depletion in the endangered Florida panther. Curr. Biol. *3*, 340–350.
17. Wildt, D.E., Bush, M., Howard, J.G., O'Brien, S.J., Meltzer, D., Van Dyk, A., Ebedes, H., and Brand, D.J. (1983). Unique seminal quality in the South African cheetah and a comparative evaluation in the domestic cat. Biol. Reprod. *29*, 1019–1025.
18. Asa, C.S. (2010). The importance of reproductive management and monitoring in canid husbandry and endangered species recovery. Int. Zoo Yearb. *44*, 102–108.
19. Snow, N.P., Andelt, W.F., and Gould, N.P. (2011). Characteristics of roadkill locations of San Clemente Island foxes. Wildl. Soc. Bull. *35*, 32–39.
20. Haller, B.C., and Messer, P.W. (2017). SLiM 2: flexible, interactive forward genetic simulations. Mol. Biol. Evol. *34*, 230–240.
21. Ohta, T. (1992). The nearly neutral theory of molecular evolution. Annu. Rev. Ecol. Syst. *23*, 263–286.
22. Westemeier, R.L., Brawn, J.D., Simpson, S.A., Esker, T.L., Jansen, R.W., Walk, J.W., Kershner, E.L., Bouzat, J.L., and Paige, K.N. (1998). Tracking the long-term decline and recovery of an isolated population. Science *282*, 1695–1698.
23. Hedrick, P.W., Peterson, R.O., Vucetich, L.M., Adams, J.R., and Vucetich, J.A. (2014). Genetic rescue in Isle Royale wolves: genetic analysis and the collapse of the population. Conserv. Genet. *15*, 1111–1121.
24. Day, S.B., Bryant, E.H., and Meffert, L.M. (2003). The influence of variable rates of inbreeding on fitness, environmental responsiveness, and evolutionary potential. Evolution *57*, 1314–1324.
25. Crnokrak, P., and Barrett, S.C. (2002). Perspective: purging the genetic load: a review of the experimental evidence. Evolution *56*, 2347–2358.
26. Xue, Y., Prado-Martinez, J., Sudmant, P.H., Narasimhan, V., Ayub, Q., Szpak, M., Frandsen, P., Chen, Y., Yngvadottir, B., Cooper, D.N., et al. (2015). Mountain gorilla genomes reveal the impact of long-term population decline and inbreeding. Science *348*, 242–245.
27. Benazzo, A., Trucchi, E., Cahill, J.A., Maisano Delser, P., Mona, S., Fumagalli, M., Bunnefeld, L., Cornetti, L., Ghirotto, S., Girardi, M., et al. (2017). Survival and divergence in a small group: the extraordinary genomic history of the endangered Apennine brown bear stragglers. Proc. Natl. Acad. Sci. USA *114*, E9589–E9597.
28. Ralls, K., and Ballou, J. (1983). Extinction: lessons from zoos. In Genetics and Conservation, C. Schonewald-Cox, S. Chambers, B. MacBryde, and L. Thomas, eds. (Benjamin/Cummings), pp. 164–184.
29. Crnokrak, P., and Roff, D.A. (1999). Inbreeding depression in the wild. Heredity *83*, 260–270.
30. Lynch, M., Conery, J., and Bürger, R. (1995). Mutational meltdowns in sexual populations. Evolution *49*, 1067–1080.
31. Gilpin, M.E., and Soulé, M.E. (1986). Minimum viable populations: processes of species extinction. In Conservation Biology: The Science of Scarcity and Diversity, M.E. Soulé, ed. (Sinauer), pp. 19–34.
32. Li, H. (2013). Aligning sequence reads, clone sequences and assembly contigs with BWA MEM. arXiv, arXiv:1303.3997v2, http://arxiv.org/abs/1303.3997v2.
33. McKenna, A., Hanna, M., Banks, E., Sivachenko, A., Cibulskis, K., Kernytsky, A., Garimella, K., Altshuler, D., Gabriel, S., Daly, M., and DePristo, M.A. (2010). The Genome Analysis Toolkit: a MapReduce framework for analyzing next-generation DNA sequencing data. Genome Res. *20*, 1297–1303.
34. Garrison, E., and Marth, G. (2012). Haplotype-based variant detection from short-read sequencing. arXiv, arXiv:1207.3907, http://arxiv.org/abs/1207.3907.
35. Zheng, X., Levine, D., Shen, J., Gogarten, S.M., Laurie, C., and Weir, B.S. (2012). A high-performance computing toolset for relatedness and principal component analysis of SNP data. Bioinformatics *28*, 3326–3328.
36. Lee, T.H., Guo, H., Wang, X., Kim, C., and Paterson, A.H. (2014). SNPhylo: a pipeline to construct a phylogenetic tree from huge SNP data. BMC Genomics *15*, 162.
37. Quinlan, A.R., and Hall, I.M. (2010). BEDTools: a flexible suite of utilities for comparing genomic features. Bioinformatics *26*, 841–842.
38. Reimand, J., Arak, T., and Vilo, J. (2011). g:Profiler—a web server for functional interpretation of gene lists (2011 update). Nucleic Acids Res. *39*, W307–W315.
39. McLaren, W., Pritchard, B., Rios, D., Chen, Y., Flicek, P., and Cunningham, F. (2010). Deriving the consequences of genomic variants with the Ensembl API and SNP Effect Predictor. Bioinformatics *26*, 2069–2070.
40. Kumar, P., Henikoff, S., and Ng, P.C. (2009). Predicting the effects of coding non-synonymous variants on protein function using the SIFT algorithm. Nat. Protoc. *4*, 1073–1081.
41. Freedman, A.H., Gronau, I., Schweizer, R.M., Ortega-Del Vecchyo, D., Han, E., Silva, P.M., Galaverni, M., Fan, Z., Marx, P., Lorente-Galdos, B., et al. (2014). Genome sequencing highlights the dynamic early history of dogs. PLoS Genet. *10*, e1004016.
42. Marsden, C.D., Ortega-Del Vecchyo, D., O'Brien, D.P., Taylor, J.F., Ramirez, O., Vilà, C., Marques-Bonet, T., Schnabel, R.D., Wayne, R.K., and Lohmueller, K.E. (2016). Bottlenecks and selective sweeps during domestication have increased deleterious genetic variation in dogs. Proc. Natl. Acad. Sci. USA *113*, 152–157.
43. Wong, A.K., Ruhe, A.L., Dumont, B.L., Robertson, K.R., Guerrero, G., Shull, S.M., Ziegle, J.S., Millon, L.V., Broman, K.W., Payseur, B.A., and Neff, M.W. (2010). A comprehensive linkage map of the dog genome. Genetics *184*, 595–605.
44. Thrall, D.E., and Robertson, I.D. (2015). Atlas of Normal Radiographic Anatomy and Anatomic Variants in the Dog and Cat, First Edition (Elsevier Saunders).
45. Pengilly, D. (1984). Developmental versus functional explanations for patterns of variability and correlation in the dentitions of foxes. J. Mammal. *65*, 34–43.
46. Trut, L.N., Oskina, I.N., and Kharlamova, A.V. (2001). Experimental studies of early canid domestication. In The Genetics of the Dog, Second Edition, E.A. Ostrander, ed. (CAB International), pp. 12–37.
47. Bouwmeester, J., Mulder, J.L., and Bree, P.V. (1989). High incidence of malocclusion in an isolated population of the red fox (*Vulpes vulpes*) in the Netherlands. J. Zool. (Lond.) *219*, 123–136.

48. Wobeser, G. (1992). Traumatic, degenerative, and developmental lesions in wolves and coyotes from Saskatchewan. J. Wildl. Dis. *28*, 268–275.

49. Harris, S. (1977). Spinal arthritis (spondylosis deformans) in the red fox, *Vulpes vulpes*, with some methodology of relevance to zooarchaeology. J. Archaeol. Sci. *4*, 183–195.

50. Porcasi, P., Porcasi, J.F., and O'Neill, C. (1999). Early Holocene coastlines of the California Bight: the Channel Islands as first visited by humans. Pac. Coast Archaeol. Soc. Q. *35*, 1–24.

51. Kim, B.Y., Huber, C.D., and Lohmueller, K.E. (2017). Inference of the distribution of selection coefficients for new nonsynonymous mutations using large samples. Genetics *206*, 345–361.

STAR★METHODS

KEY RESOURCES TABLE

REAGENT or RESOURCE	SOURCE	IDENTIFIER
Biological Samples		
Island and gray fox DNA samples	Archive of RKW	See Table S1
Island and gray fox skulls and skeletons	Museum collections	See table: https://doi.org/10.5281/zenodo.1345794
Deposited Data		
Raw whole genome sequence reads	[5] and this study	BioProjects PRJNA312115, PRJNA478450
Table of morphological data	This study	https://doi.org/10.5281/zenodo.1345794
Software and Algorithms		
msprime v0.5.0	[11]	https://pypi.org/project/msprime/
SLiM v2.4.2	[20]	https://messerlab.org/slim/
BWA MEM v0.7.7-r441	[32]	http://bio-bwa.sourceforge.net/
GATK v3.7-0-gcfedb67	[33]	https://software.broadinstitute.org/gatk/
FreeBayes v1.1.0-3-g961e5f3	[34]	https://github.com/ekg/freebayes
SNPRelate v1.12.2	[35]	https://doi.org/10.18129/B9.bioc.SNPRelate
SNPhylo v20140701	[36]	https://github.com/thlee/SNPhylo
BedTools v2.26.0	[37]	https://github.com/arq5x/bedtools2
gProfileR v0.6.1	[38]	http://cran.r-project.org/web/packages/gProfileR/
VEP with SIFT option v87	[39, 40]	https://www.ensembl.org/vep
Scripts for island fox simulations	This study	https://doi.org/10.5281/zenodo.1345812

CONTACT FOR REAGENT AND RESOURCE SHARING

Further information and requests for resources and reagents should be directed to and will be fulfilled by the Lead Contact, Jacqueline Robinson (jacqueline.robinson@ucsf.edu).

EXPERIMENTAL MODEL AND SUBJECT DETAILS

DNA samples from island foxes sampled in 2000-2009 from each population and from a Northern California gray fox were obtained from the archive of Dr. Robert K. Wayne for whole genome sequencing on Illumina HiSeq machines at the Vincent J. Coates Genomics Sequencing Laboratory at the University of California, Berkeley. Additionally, we sequenced DNA isolated from miscellaneous bone fragments from a San Nicolas island fox specimen collected in 1929 (#15477, Donald R. Dickey Collection, University of California, Los Angeles). Finally, we generated new higher quality sequence data from a 1988 Santa Rosa island fox, as the Santa Rosa genome from Robinson et al. [5] was of relatively low quality compared to the other sequences. Further sample details are provided in Table S1. We incorporated the genomes from Robinson et al. [5] yielding a total of 16 genomes at 13-23X coverage.

METHOD DETAILS

Read alignment and processing followed the methods outlined in Robinson et al. [5]. Briefly, reads were aligned to the domestic dog reference genome, canFam3.1, with BWA MEM [32], followed by removal of duplicate and low quality reads (reads with mapping quality Phred score < 30 and reads not mapped in proper pairs), base quality score recalibration with the Genome Analysis Toolkit (GATK [33]), joint genotyping with FreeBayes [34], and finally variant and genotype filtering. Variants that were not biallelic SNPs with Phred score $\geq$30, variant sites with more than 4 missing genotypes, and variant sites with more than 75% of genotypes called as heterozygous were filtered out. Heterozygous genotypes at sites with skewed allele balance (<0.2 or >0.8) were also excluded. Sites in CpG islands, repetitive regions, or with excess depth (>99th percentile total depth) were masked. At least two observations of the alternate allele on each of the forward and reverse strands were required as evidence of a variant site. Further, genotypes with fewer than 6 supporting reads, with Phred score less than 20, or with depth greater than the 99th percentile for a given individual were filtered out.

QUANTIFICATION AND STATISTICAL ANALYSIS

Analysis of variation in island and gray fox genomes

We evaluated the genetic distance between individuals with a maximum-likelihood phylogenetic tree and principal components analysis (PCA), both based on a set of 12,249 SNPs pruned for linkage disequilibrium (maximum = 0.2) with a minimum minor allele frequency of 0.1 and no missing data. The pruning and PCA were conducted with SNPRelate [35]. The tree was generated in SNPhylo from 1,000 bootstrap replicates [36].

We assessed genetic diversity by calculating heterozygosity, here defined as the number of heterozygous genotypes divided by the number of called sites within a single individual. Heterozygosity was calculated for the entire autosomal genome and in 100 kb sliding windows with a 10 kb step size. Windows with more than 20% of sites failing quality filters, or with fewer than 20 kb of confidently called sequence were excluded. Peaks of heterozygosity within a genome were defined as windows with heterozygosity greater than two standard deviations above the mean, based on the genome-wide distribution of per-window heterozygosity. Overlapping windows of high heterozygosity were merged using BEDTools [37]. Peaks were assessed for putative functional relevance by conducting a gene ontology enrichment analysis in gProfileR [38]. The g:SCS correction method within gProfileR was used to assess significance.

Since analysis of olfactory receptor genes may be complicated by their elevated rate of evolution, which could produce technical artifacts due to improper read alignment, we employed several stringent filters (described above) that should reduce the inclusion of likely gene paralogs in our analyses. These filters excluded regions of excessive depth (indicating possible gene copy number differences) and low sequence complexity (indicating repetitive or non-unique sequence), reads with low mapping quality (indicating non-unique alignment or excessive mismatches to the reference), variants with skewed allele balance in heterozygotes or excess heterozygosity, and windows with a large fraction of sites failing filters. Manual inspection of a subset of San Nicolas heterozygous peak regions revealed few that were obviously the result of alignment errors, although this possibility cannot be ruled out with the existing data. We confirmed that technical differences were not driving variation in peaks containing OR genes between San Nicolas genomes by determining that >98% of peaks overlapping OR genes were confidently called across all four individuals.

Coordinates of the set of 13,647 putatively neutral 1-kb loci in the dog reference genome were those employed by Robinson et al. ([5], originally from [41]). These regions were designed to be distant from functional regions ($\geq$10 kb from coding sequence, $\geq$100 bp from conserved non-coding sequence) while excluding regions likely to have problematic alignment due to repetitive content or low mappability, and were spaced $\geq$ 30 kb apart to reduce the effects of non-independence due to linkage. Coordinates of zero-fold degenerate sites (where all mutations are amino acid-changing) and four-fold degenerate sites (where all mutations result in the same amino acid) within protein-coding regions were those employed by Robinson et al. ([5], originally from [42]). Levels of deleterious variation were evaluated by calculating the proportion of derived alleles per genome at synonymous and non-synonymous sites in coding regions as follows.

Variant annotation was conducted with Ensembl's Variant Effect Predictor (VEP [39]) and the Sorting Intolerant From Tolerant (SIFT [40]) tool. SIFT classifies non-synonymous mutations at each site as likely to be deleterious or tolerated on the basis of amino acid conservation across taxa. Following Robinson et al. [5], likelihood ratio tests were used to evaluate whether the proportion of homozygotes and the proportion of derived alleles differed significantly between gray and island foxes at synonymous, tolerated, deleterious, and LOF variant sites. The test compared the likelihoods under two models; under the null model, there is a single mean value (q) for all gray and island foxes, and under the alternative model, the island fox mean (q_i) may differ from the gray fox mean (q_g). Log-likelihood values for the null and alternative models were used to calculate the likelihood ratio test statistic, $\Lambda = -2(\text{log-likelihood}_{\text{null}} - \text{log-likelihood}_{\text{alternative}})$. Asymptotically, Λ is χ^2-distributed with one degree of freedom. This distribution was used to calculate p values. For allele tests, the null model assumes the ratio of q_i to q_g found at synonymous SNPs. This is a conservative test of whether the difference in the proportion of derived alleles between island and mainland foxes is greater than that seen at synonymous SNPs, which should be equivalent under neutrality, but was found to differ slightly, reflecting possible technical biases such as the under-calling of heterozygotes.

Coalescent simulations under San Nicolas demographic models

We performed neutral coalescent simulations in msprime [11] under plausible models of San Nicolas demographic history to evaluate empirical patterns of genome-wide diversity in this population. The parameters of demographic models inferred in Robinson et al. [5] were used. Briefly, these parameters were obtained through approximate Bayesian computation, and were designed to match observed levels of heterozygosity within 13,647 putatively neutral 1-kb loci (described above) in the 1988 San Nicolas genome. Parameter values from the 100 models with the best fit to the empirical data constituted the posterior distribution. Here, we sampled parameters with replacement from the joint posterior distribution 1,000 times to simulate complete San Nicolas genomes under neutrality. The simulated genomes consisted of 220 ''chromosomes'' of 10 Mb in length to emulate the size of the autosomal dog reference genome. We used a mutation rate of 2×10^{-8} per site per generation, and assumed a generation time of one year. A single per-site recombination rate was randomly sampled for each chromosome, drawn from the recombination rates inferred in a study in dogs [43]. The genome architecture, mutation rate, and recombination rates were chosen to be consistent with Robinson et al. [5].

Within each simulation, we randomly sampled one individual in the generation corresponding to the year 1929, two individuals in 1988, and one individual in 2000, and obtained the coordinates of peaks of heterozygosity within these genomes as we did in our analysis of the empirical data. Specifically, we calculated heterozygosity in 100 kb windows with a 10 kb step size for each individual.

To take into account the variance in missing data rates across windows in the sequenced genomes, we randomly selected a subset of sites within each simulated window to match the number of sites observed empirically in each San Nicolas genome. Overlapping windows were merged prior to calculating the number of peaks of heterozygosity, the mean width of peaks of heterozygosity, and the proportion of unique peaks within each individual. To determine whether the empirical values we obtained from the sequenced genomes were expected based on the simulated results, we calculated the percentile rankings of where the empirical values fell within the distributions obtained from simulation. In all cases, the empirical values fell within the middle 95% interval of the simulated statistics, implying that the empirical results are expected under neutrality in San Nicolas demographic models.

Morphological assay of gray and island fox museum specimens

Skulls (n = 141) and complete skeletons (n = 163) of adult gray and island foxes sampled between 1929 and 2013 were obtained from collections in the Los Angeles County Museum of Natural History, the Santa Barbara Museum of Natural History, and the Donald Ryder Dickey Bird and Mammal Collection at the University of California, Los Angeles. Specimens were placed in anatomical position and surveyed for skeletal abnormalities including irregular development, healed fracture, and bony growths (from infection, muscle traction or other causes). Vertebrae were identified and counted with the exception of distal caudal vertebrae, which were missing from many specimens, and are also variable between islands. Specimen information and morphological descriptions are available in a table archived at https://doi.org/10.5281/zenodo.1345794.

We defined "congenital" abnormalities as pathologies of the axial skeleton not related to trauma or injury. Observed congenital defects included extra vertebrae, transitional vertebrae (LSTV: malformed final lumbar vertebra with characteristics of a sacral vertebra, SCTV: malformed final sacral vertebra with characteristics of a caudal vertebra), and maloccluded teeth. LSTV is implicated in function impairment but SCTV has no clinical significance [15, 44]. Malocclusion has been found to have a significant genetic component in small canids generally [45, 46] and in reproductively isolated fox (*Vulpes vulpes*) populations specifically [47]. A genetic basis has not been established for extra vertebrae or transitional vertebrae, but the high incidence of congenital vertebral anomalies in highly inbred wolf populations on Isle Royale and in Scandinavia implies that there is a heritable component in canids [14, 15]. Vertebral abnormalities are absent or rare in outbred wolf and coyote (*Canis latrans*) populations that have been surveyed [14, 15, 48].

We binned traumatic pathologies into a broad category of "trauma" and a more conservative category of trauma resulting from collision with a vehicle. Injury pathologies were broadly defined to include fracture, infection, osteoarthritis, osteophytes and evidence of abnormal muscle use (e.g., traction, roughened insertion). Only healed injuries were recorded, thus all foxes obtained as traffic fatalities were counted only if they had previously survived a collision. Thus, the frequency of vehicle collision rates is an underestimate. To identify probable vehicle collisions, we expanded the diagnosis of Harris [49] in which multiple bones from the same side of the body were fractured, particularly in the hindlimb and ribs. In our analyses, evidence of muscular strain on the same side as multiple fractured elements were included as evidence of trauma to that side of the body, since we surveyed animals that survived collisions but Harris necropsied fresh traffic fatalities.

Fisher's exact test was used to test for significant differences in the prevalence of congenital and traumatic pathologies between island and mainland foxes. Additionally, relative risk scores for congenital and traumatic pathologies were calculated for all population pairs. The relative risk score is the ratio of the incidence of pathology between two populations, where incidence is defined as the number of individuals with the pathology divided by the number of individuals examined. For example, if the incidence of pathology in one population is 1/10, and the incidence in a second population is 2/50, the relative risk of pathology in the first population relative to the second is 0.1/0.04 = 2.5; likewise the relative risk in the second population relative to the first is 0.04/0.1 = 0.4. Statistical significance was determined by calculating relative risk scores in 1,000 permutations where population labels were assigned to specimens at random. Empirical relative risk scores greater than the 95th percentile of scores obtained through permutation were deemed significant.

Forward simulations of genetic variation in island versus mainland populations

We simulated neutral and deleterious variation under six different demographic models, each involving the establishment of a small island population (N = 1,000, 500, 200, 100, or 50 individuals) from a large mainland population (N = 10,000 individuals) to evaluate the possibility of purging in island populations. Simulations were conducted with SLiM [20]. In the most basic model (Split Model), an island population of is established by sampling individuals from the mainland population with replacement, such that the mainland population is unaffected by the formation of the island population. The mainland population was kept at constant size for 10,000 generations. A range of island population sizes was chosen because census sizes of island fox populations vary from a few hundred to just under 2,000 individuals per island [8]. Recent estimates suggest an initial colonization of the islands by foxes at ~9,200 years BP [4], and we assumed a one-year generation time. The purpose of the basic split model was to compare a small population against a larger one, without any additional complexities (e.g., inbreeding).

The other five models are variations on the split model, reflecting plausible elements of island fox history, specifically: 1) an ancient bottleneck to simulate a small founding population (Ancient Bottleneck Model); 2) a recent bottleneck 30 generations ago, such as may have occurred in San Nicolas during the 1970s [10] (Recent Bottleneck Model); 3) a serial bottleneck (at 10,000 and 2,000 generations ago) to mimic the possibility of serial colonization of the Northern and then the Southern Channel Islands (Serial Bottleneck Model); 4) a model in which the island population is initially large (N = 2,000 for ~2,000 generations), as may have occurred if the foxes initially the Northern Channel Islands when they constituted a single landmass (Santarosae) when sea levels were lower > 10,000 years ago [50] (Big Island Model); and 5) a model with recent strong inbreeding, where individuals are twice as likely to mate with

close relatives than non-kin (Inbreeding Model). All bottlenecks consist of a starting population of ten individuals that doubles in size each generation until the final population size (1,000, 500, 200, 100, or 50 individuals) is reached.

Each simulated individual consists of a diploid 2 Mb genome, consisting of 2,000 "genes" carried on 38 chromosomes proportional to chromosome lengths in the dog genome. Note that this number of genes is approximately 1/10th the number found in the dog genome. Each gene was represented by a contiguous 1 kb sequence that accumulated mutations at a rate of 1×10^{-8} per nucleotide per generation. 30% of these mutations were selectively neutral, and the remaining 70% were deleterious, with selection coefficients drawn from a gamma distribution of fitness effects [51]. Recombination was incorporated by including a single base pair in between each gene that did not accumulate mutations, but where crossovers occurred at a rate of 1×10^{-3} per site per generation. This was done to mimic intergenic regions 100 kb in length with a recombination rate of 1×10^{-8} per site per generation without simulating extraneous non-coding sequence. Each model was run for 10,000 generations following a 100,000-generation burn-in period.

The average number of alleles and the average number of homozygous alleles carried by each individual were calculated for deleterious ($s < 0$) and neutral mutations ($s = 0$). We grouped deleterious mutations arbitrarily as strongly ($s < -0.01$), moderately ($-0.01 \leq s < -0.001$), and weakly deleterious ($-0.001 \leq s < 0$). We categorized deleterious mutations by selection coefficient (s), rather than population-rescaled coefficients (Ns), specifically to explore the effects of different population sizes on the accumulation/depletion of mutations with non-zero selection coefficients. Within a simulation, deleterious mutations were either entirely additive ($h = 0.5$) or entirely recessive ($h = 0.0$). Fifty replicates were performed for each dominance value and each island size (N = 1,000, 500, 200, 100, or 50) under each of the six models (3,000 simulations total). One-way ANOVA and Tukey HSD post hoc tests were used to evaluate significant differences in the number of total alleles and the number of homozygous alleles between different models.

DATA AND SOFTWARE AVAILABILITY

All newly generated raw whole genome sequence reads have been deposited in the NCBI Sequence Read Archive under BioProject PRJNA478450. Previously sequenced reads from Robinson et al. [5] are available under BioProject PRJNA312115. A table containing museum specimen information and phenotypic descriptions used for the morphological assessment is available at https://doi.org/10.5281/zenodo.1345794. Scripts for coalescent and forward simulations are available at https://github.com/jarobin/islandfox2018, and archived at https://doi.org/10.5281/zenodo.1345812.

Current Biology, Volume *28*

Supplemental Information

Purging of Strongly Deleterious Mutations Explains Long-Term Persistence and Absence of Inbreeding Depression in Island Foxes

Jacqueline A. Robinson, Caitlin Brown, Bernard Y. Kim, Kirk E. Lohmueller, and Robert K. Wayne

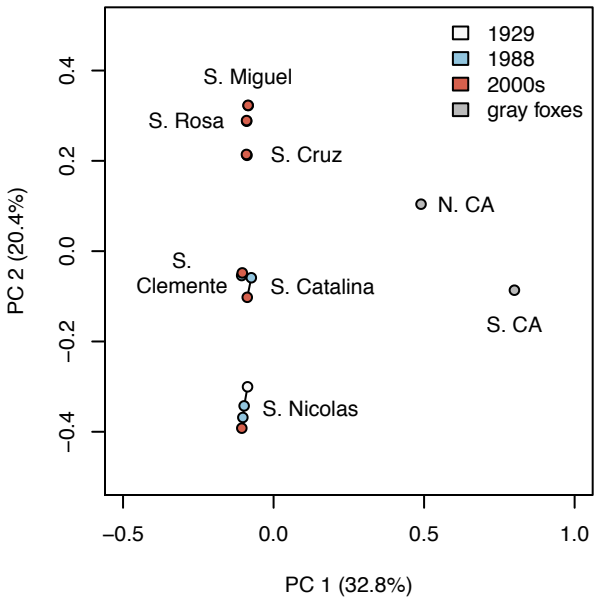

Figure S1. Principal component analysis of gray and island fox genomes. Related to Figure 1. Based on 12,249 SNPs pruned for linkage disequilibrium. Solid black lines connect points from the same population.

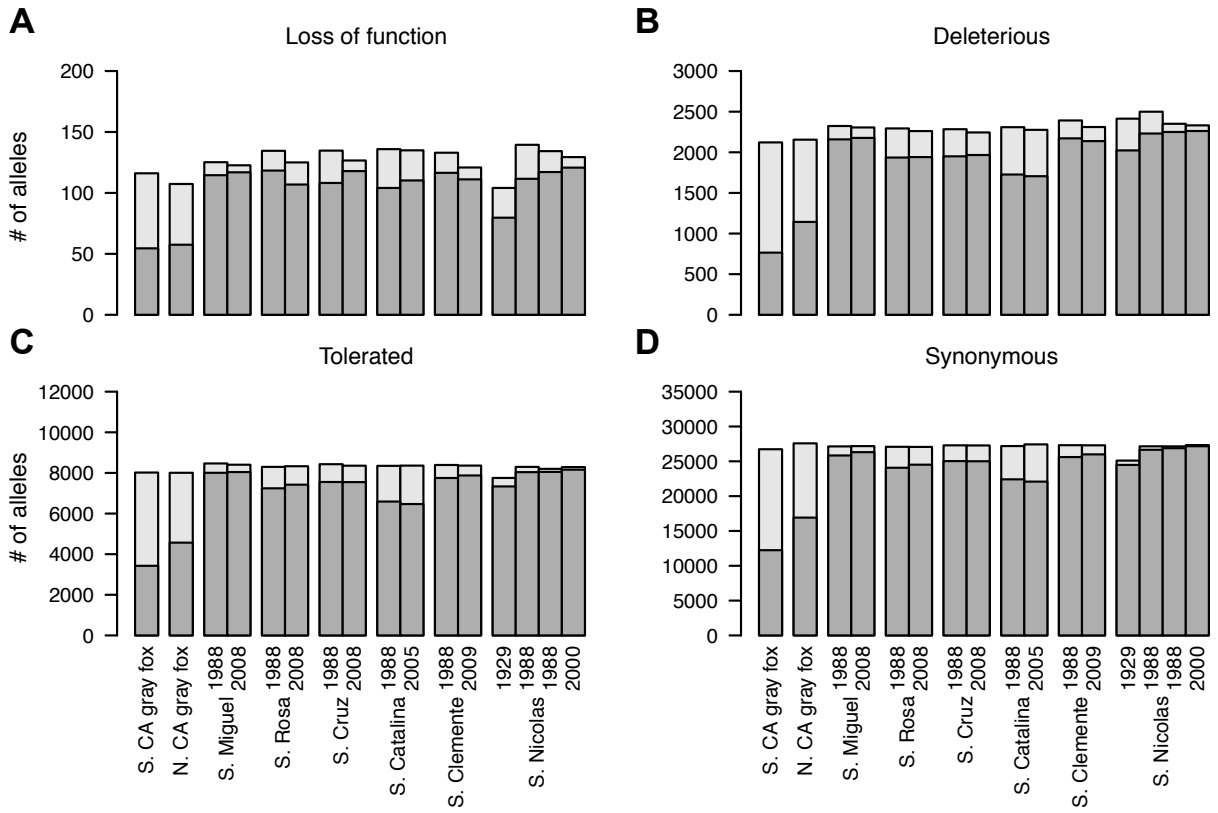

Figure S2. Number of derived alleles in island and gray fox coding regions. Related to Figure 2. The number of derived alleles contained in homozygous genotypes in each individual is shown in dark grey, and the total number of derived alleles in light grey. The homozygosity and total number of derived alleles is elevated at putatively deleterious variant sites in island fox genomes (see Table S4). Mutations are classified by annotation type by the Ensembl Variant Effect Predictor [VEP; S1] and the Sorting Intolerant From Tolerant algorithm [SIFT; S2]. Numbers within each category are normalized by the mean number of genotyped sites across individuals to account for differences in coverage between individuals. (*A*) Loss of function mutations are those that encode premature stop codons. (*B*, *C*) Deleterious and tolerated mutations are missense mutations categorized by SIFT [S2] according to whether they are predicted to be damaging. (*D*) Synonymous changes are mutations that do not change the encoded amino acid and are presumed to be neutral.

Species	Location	Sample #	Sex	Year Sampled	Platform	Base Pairs (Gbp)	# of reads aligned, post-filtering ($x 10^6$)	Mean depth of coverage (X)	Source
ULI	Santa Catalina	SCA16/ RKW4644	F	1988	HiSeq2000, 2x100bp	82.5	311	12.8	[S3]
ULI	San Clemente	SCLV4/ RKW4045	F	1988	HiSeq2000, 2x100bp	73.2	450	18.7	[S3]
ULI	Santa Cruz	SCZ05/ RKW12331	M	1988	HiSeq2000, 2x100bp	77.9	348	14.5	[S3]
ULI	San Miguel	SMI15/ RKW12354	F	1988	HiSeq2000, 2x100bp	80.5	559	23.2	[S3]
ULI	San Nicolas	SNI05/ RKW4038	F	1988	HiSeq2000, 2x100bp	66.1	339	13.8	[S3]
ULI	San Nicolas	SNI41/ RKW12349	F	1988	HiSeq2000, 2x100bp	84.3	328	13.6	[S3]
UCI	SMMNRA	NPS GFO41	F	2012	HiSeq2000, 2x100bp	67.5	409	17.0	[S3]
ULI	Santa Catalina	RKW11697	M	2005	HiSeq4000, 2x100bp	70.8	526	22.3	This study
ULI	San Clemente	RKW13704	F	2009	HiSeq4000, 2x100bp	69.5	442	18.7	This study
ULI	Santa Cruz	RKW8695	F	2008	HiSeq4000, 2x100bp	72.3	511	21.7	This study
ULI	San Miguel	RKW11655	M	2008	HiSeq4000, 2x100bp	69.6	516	21.9	This study
ULI	San Nicolas	RKW12297	M	2000	HiSeq4000, 2x100bp	73.0	492	20.9	This study
ULI	San Nicolas	Dickey 15477	F	1929	HiSeq4000, 1x100bp	118.5	478	15.8	This study
ULI	Santa Rosa	SRO13/ RKW12355	F	1988	HiSeq4000, 2x100bp	76.0	527	22.2	This study
ULI	Santa Rosa	RKW10660	M	2008	HiSeq4000, 2x100bp	78.0	534	22.7	This study
UCI	GOGANRA	NPS GFO30	M	1993	HiSeq4000, 2x100bp	70.6	446	18.8	This study

Table S1. Sample information and metrics for genome sequences. Related to Figure 1. ULI: *Urocyon littoralis*; UCI: *Urocyon cinereoargenteus*; SMMNRA: Santa Monica Mountains National Recreation Area; GOGANRA: Golden Gate National Recreation Area. In the main text and supplemental items, San Nicolas 1988 (1) refers to SNI05/RKW4038 and San Nicolas 1988 (2) refers to SNI41/RKW12349. All raw sequence reads are available for download from the NCBI Sequence Read Archive. Sequences from Robinson et al. 2016 [S3] can be found under BioProject PRJNA312115, and sequences generated for this study can be found under PRJNA478450.

Statistic	Empirical value	Empirical percentile	Simulated mean	Simulated 2.5th percentile	Simulated 97.5th percentile
Number of peaks in 1929 genome	122	89.2	99.7	22	498
Number of peaks in 1988 (1) genome	140	91.2	98.9	20	655
Number of peaks in 1988 (2) genome	94	87.7	95.4	20	729
Number of peaks in 2000 genome	92	86.9	97	20	644
Mean peak width in 1929 genome	204.5 kb	13.1	312.7 kb	134.5 kb	570.5 kb
Mean peak width in 1988 (1) genome	186.0 kb	20.8	289.2 kb	127.9 kb	549.7 kb
Mean peak width in 1988 (2) genome	216.4 kb	19.3	294.6 kb	128.8 kb	607.1 kb
Mean peak width in 2000 genome	199.5 kb	20.2	289.3 kb	128.6 kb	539.2 kb
Proportion of shared peaks in 1929 genome	0.415	15.9	0.537	0.293	0.761
Proportion of shared peaks in 1988 (1) genome	0.687	27.3	0.731	0.311	0.919
Proportion of shared peaks in 1988 (2) genome	0.869	86.7	0.731	0.344	0.939
Proportion of shared peaks in 2000 genome	0.754	46.9	0.732	0.312	0.918
Proportion of peaks shared by 2+ individuals among all 4 San Nicolas genomes	0.439	15.4	0.729	0.346	0.789

Table S2. Statistics related to peaks of heterozygosity in empirical and simulated San Nicolas fox genomes. Related to Figure 1. No empirical values fall outside of the middle 95% of values obtained through simulation.

Individual	Enrichment *p*-value	GO Term	Description
S. CA Gray Fox (1932 genes in 861 peaks)	1.29E-16	GO:0050911	Detection of chemical stimulus involved in sensory perception of smell
	1.46E-11	GO:0007186	G-protein coupled receptor signaling pathway
	6.84E-11	GO:0005886	Plasma membrane
	0.00576	GO:0045095	Keratin filament
	0.0163	GO:0000786	Nucleosome
	0.00556	GO:0005549	Odorant binding
	1.29E-16	GO:0004984	Olfactory receptor activity
	0.0103	HP:0005356	Decreased serum complement factor I
	0.0432	KEGG:04610	Complement and coagulation cascades
	1.43E-16	KEGG:04740	Olfactory transduction
N. CA Gray Fox (2897 genes in 1109 peaks)	0.014	GO:0018101	Protein citrullination
	0.00108	GO:0071944	Cell periphery
	3.90E-13	GO:0005882	Intermediate filament
	0.00317	GO:0016021	Integral component of membrane
	0.014	GO:0004668	Protein-arginine deiminase activity
	0.0209	GO:0060089	Molecular transducer activity
	0.00498	KEGG:04740	Olfactory transduction
S. Catalina 1988 (3539 genes in 1213 peaks)	0.0477	GO:0098662	Inorganic cation transmembrane transport
	0.0331	GO:0045095	Keratin filament
	0.000906	GO:0016021	Integral component of membrane
S. Catalina 2005 (3830 genes in 1349 peaks)	1.23E-29	GO:0050906	Detection of stimulus involved in sensory perception
	0.00278	GO:1900543	Negative regulation of purine nucleotide metabolic process
	1.65E-05	GO:0005882	Intermediate filament
	1.32E-13	GO:0005886	Plasma membrane
	4.66E-06	GO:0005549	Odorant binding
	1.52E-29	GO:0004984	Olfactory receptor activity
	0.00587	GO:0004064	Arylesterase activity
	3.64E-25	KEGG:04740	Olfactory transduction
	0.00371	KEGG:04610	Complement and coagulation cascades
S. Clemente 1988 (2697 genes in 643 peaks)	NA	NA	NA
S. Clemente 2009 (2342 genes in 617 peaks)	NA	NA	NA
S. Cruz 1988 (3630 genes in 1203 peaks)	0.00413	KEGG:04924	Renin secretion
	0.0295	KEGG:04713	Circadian entrainment
S. Cruz 2008 (3575 genes in 1253 peaks)	0.0222	GO:0007399	Nervous system development
	0.027	GO:0048856	Anatomical structure development
	0.0143	GO:0008146	Sulfotransferase activity
S. Miguel 1988 (2506 genes in 614 peaks)	NA	NA	NA

S. Miguel 2008 (1966 genes in 431 peaks)	5.56E-06	GO:0045095	Keratin filament
	0.0454	HP:0010669	Hypoplasia of the zygomatic bone
	0.0428	HP:0002253	Colonic diverticula
	0.0106	HP:0004428	Elfin facies
	0.0129	HP:0000796	Urethral obstruction
	0.00157	HP:0100025	Overfriendliness
	0.001	HP:0002623	Overriding aorta
	0.042	HP:0010780	Hyperacusis
	0.00157	HP:0001361	Nystagmus-induced head nodding
	0.042	HP:0100817	Renovascular hypertension
	0.000385	HP:0007720	Flat cornea
	0.0227	HP:0000015	Bladder diverticulum
	0.0221	HP:0002183	Phonophobia
S. Nicolas 1929 (531 genes in 122 peaks)	2.55E-07	GO:0007186	G-protein coupled receptor signaling pathway
	5.38E-17	GO:0007608	Sensory perception of smell
	5.59E-17	GO:0004984	Olfactory receptor activity
	0.00578	GO:0005549	Odorant binding
	3.57E-16	KEGG:04740	Olfactory transduction
S. Nicolas 1988 (1) (626 genes in 140 peaks)	0.0229	GO:0035095	Behavioral response to nicotine
	5.61E-31	GO:0007186	G-protein coupled receptor signaling pathway
	1.15E-43	GO:0050907	Detection of chemical stimulus involved in sensory perception
	3.79E-12	GO:0016021	Integral component of membrane
	0.000464	GO:0004252	Serine-type endopeptidase activity
	2.36E-05	GO:0003823	Antigen binding
	0.00943	GO:0004497	Monooxygenase activity
	0.0126	GO:0016705	Oxidoreductase activity, acting on paired donors, with incorporation or reduction of molecular oxygen
	2.94E-43	GO:0004984	Olfactory receptor activity
	0.0259	GO:0005549	Odorant binding
	8.42E-31	KEGG:04740	Olfactory transduction
S. Nicolas 1988 (2) (440 genes in 94 peaks)	8.05E-19	GO:0007608	Sensory perception of smell
	0.0036	GO:0035095	Behavioral response to nicotine
	0.00871	GO:0016021	Integral component of membrane
	0.021	GO:0005886	Plasma membrane
	1.16E-18	GO:0004984	Olfactory receptor activity
	2.21E-09	GO:0005149	Interleukin-1 receptor binding
	0.0241	GO:0004252	Serine-type endopeptidase activity
	0.0496	HP:0002654	Multiple epiphyseal dysplasia
	2.78E-15	KEGG:04740	Olfactory transduction
S. Nicolas 2000 (379 genes in 92 peaks)	0.00689	GO:0051716	Cellular response to stimulus
	7.45E-26	GO:0050907	Detection of chemical stimulus involved in sensory perception
	6.62E-19	GO:0007186	G-protein coupled receptor signaling pathway

	0.0253	GO:0031224	Intrinsic component of membrane
	7.46E-09	GO:0005549	Odorant binding
	0.000212	GO:0004252	Serine-type endopeptidase activity
	7.43E-25	GO:0004984	Olfactory receptor activity
	3.79E-20	KEGG:04740	Olfactory transduction
S. Rosa 1988 (3715 genes in 1235 peaks)	0.00932	KEGG:00590	Arachidonic acid metabolism
S. Rosa 2008 (3735 genes in 1209 peaks)	0.018	GO:0044763	Single-organism cellular process
	0.0218	GO:0051216	Cartilage development
	0.0389	GO:0048149	Behavioral response to ethanol
	0.000344	GO:0005887	Integral component of plasma membrane
	0.0329	GO:0004499	N,N-dimethylaniline monooxygenase activity
	0.000802	KEGG:04080	Neuroactive ligand-receptor interaction

Table S3. Gene ontology enrichment results for peaks of heterozygosity in island and gray fox genomes. Related to Figure 1. Only terms with significant enrichment *p*-values (<0.05) are shown.

Type	Null model MLE	Alternative model MLE	Likelihood ratio test
Proportion of Homozygous Derived Genotypes (Gray Foxes v. 1988-2009 Island Foxes)			
Synonymous	$q_i=q_g$=0.320	q_i=0.339, q_g=0.196	Λ=6692.54, $\mathbf{p<<10^{-16}}$
Tolerated	$q_i=q_g$=0.279	q_i=0.298, q_g=0.157	Λ=2480.20, $\mathbf{p<<10^{-16}}$
Deleterious	$q_i=q_g$=0.208	q_i=0.224, q_g=0.104	Λ=808.49, $\mathbf{p<<10^{-16}}$
Loss of function	$q_i=q_g$=0.234	q_i=0.251, q_g=0.124	Λ=40.44, $\mathbf{p=2.03 \times 10^{-10}}$
Proportion of Derived Alleles (Gray Foxes v. 1988-2009 Island Foxes)			
Tolerated	$q_i=1.002435q_g$, q_g=0.326	q_i=0.328, q_g=0.315	Λ=31.60, $\mathbf{p=1.89 \times 10^{-8}}$
Deleterious	$q_i=1.002435q_g$, q_g=0.251	q_i=0.254, q_g=0.234	Λ=32.72, $\mathbf{p=1.06 \times 10^{-8}}$
Loss of function	$q_i=1.002435q_g$, q_g=0.282	q_i=0.289, q_g=0.247	Λ=6.76, $\mathbf{p=9.33 \times 10^{-3}}$
Proportion of Derived Alleles (Gray Foxes v. 1988 Island Foxes)			
Tolerated	$q_i=1.001165q_g$, q_g=0.325	q_i=0.328, q_g=0.315	Λ=30.20, $\mathbf{p=3.90 \times 10^{-8}}$
Deleterious	$q_i=1.001165q_g$, q_g=0.252	q_i=0.254, q_g=0.234	Λ=40.56, $\mathbf{p=1.91 \times 10^{-10}}$
Loss of function	$q_i=1.001165q_g$, q_g=0.285	q_i=0.289, q_g=0.247	Λ=8.53, $\mathbf{p=3.50 \times 10^{-3}}$
Proportion of Derived Alleles (Gray Foxes v. 2000-2009 Island Foxes)			
Tolerated	$q_i=1.003915q_g$, q_g=0.324	q_i=0.328, q_g=0.315	Λ=25.40, $\mathbf{p=4.66 \times 10^{-7}}$
Deleterious	$q_i=1.003915q_g$, q_g=0.246	q_i=0.254, q_g=0.234	Λ=18.24, $\mathbf{p=1.95 \times 10^{-5}}$
Loss of function	$q_i=1.003915q_g$, q_g=0.271	q_i=0.289, q_g=0.247	Λ=3.67, $p=5.56 \times 10^{-2}$

Table S4. Comparisons of the proportion of homozygous derived genotypes and the proportion of derived alleles per individual between gray and island foxes. Related to Figure 2. Significant *p*-values (<0.05) are in bold.

	S. Catalina	S. Clemente	S. Cruz	S. Miguel	S. Nicolas	S. Rosa	Gray Fox
S. Catalina		2.00	*Inf*	2.58	7.33	2.50	3.75
S. Clemente	1.60		NA	1.55	3.20	1.30	1.88
S. Cruz	*Inf*	*Inf*		0	0	0	0
S. Miguel	10.33*	7.75*	0		2.06	0.640	1.03
S. Nicolas	1.30	0.977	0	0.176*		0.312	2.13
S. Rosa	NA	NA	NA	*Inf*	*Inf*		0.660
Gray Fox	*Inf**	*Inf**	NA	0	0	NA	

Table S5. Relative risks of developmental and probable collision pathologies between island foxes and mainland gray fox morphological samples. Related to Figure 3. Relative risks of developmental pathologies are above the diagonal and relative risks of probable collision pathologies are below the diagonal. The table is read: *Row* has X times the risk of pathology as *Column*. A zero represents no risk relative to the column; "*Inf*" represents cases where the column had no reported cases and the risk in the row population is thus infinitely greater. For collision pathologies, a comparison is not available (NA) between samples where neither sample contained probable collision pathologies. Asterisks denote risks significant below a 0.05 threshold based on the permutation test. For developmental pathologies, no relative risk results were statistically significant.

Selection Strength (s)	N_{island}	Additive Regime						Recessive Regime					
		Split	Big Island	Ancient Bottleneck	Serial Bottleneck	Recent Bottleneck	Inbreeding	Split	Big Island	Ancient Bottleneck	Serial Bottleneck	Recent Bottleneck	Inbreeding
[-1, -0.1)	1000	0.875	1.14	1.15	1.10	0.963	0.984	***0.400***	***0.395***	***0.391***	***0.314***	***0.255***	***0.138***
	500	1.06	1.27	0.941	1.07	0.904	0.648	***0.259***	***0.268***	***0.217***	***0.251***	***0.201***	***0.0836***
	200	1.19	1.30	0.850	1.05	0.718	1.61	***0.131***	***0.176***	***0.154***	***0.182***	***0.0965***	***0.0777***
	100	0.646	0.812	1.79	0.971	0.630	1.14	***0.143***	***0.0882***	***0.0677***	***0.0549***	***0.145***	***0.0492***
	50	0.450	1.97	1.60	1.91	3.15	2.47	***0.0799***	***0.127***	***0.122***	***0.0750***	***0.0507***	***0.0172***
[-0.1, -0.01)	1000	1.03	0.953	1.00	1.05	1.17	1.03	***0.330***	***0.349***	***0.335***	***0.330***	***0.341***	***0.266***
	500	1.17	1.02	1.08	1.03	1.29	0.928	***0.241***	***0.238***	***0.267***	***0.260***	***0.253***	***0.216***
	200	***2.19***	1.69	2.04	***2.24***	***2.67***	1.95	***0.316***	***0.255***	***0.304***	***0.286***	***0.298***	***0.233***
	100	***9.55***	***8.39***	***9.05***	***9.16***	***11.0***	***9.89***	1.04	***0.742***	0.905	0.905	0.906	0.962
	50	***26.6***	***22.8***	***27.6***	***29.8***	***28.2***	***29.1***	***2.36***	***1.95***	***2.39***	***2.25***	***2.26***	***2.45***
[-0.01, -0.001)	1000	***1.74***	***1.63***	***1.87***	***1.88***	***1.76***	***1.74***	***0.630***	***0.605***	***0.651***	***0.682***	***0.609***	***0.605***
	500	***3.51***	***3.18***	***3.29***	***3.58***	***3.31***	***3.25***	1.02	***0.867***	1.01	0.993	0.998	1.00
	200	***7.03***	***6.16***	***6.82***	***7.00***	***6.72***	***6.57***	***1.74***	***1.42***	***1.75***	***1.79***	***1.77***	***1.81***
	100	***9.65***	***8.36***	***9.46***	***9.48***	***10.3***	***9.73***	***2.34***	***1.82***	***2.30***	***2.36***	***2.27***	***2.26***
	50	***11.3***	***9.87***	***11.8***	***12.1***	***11.8***	***12.1***	***2.66***	***2.20***	***2.71***	***2.67***	***2.61***	***2.63***
[-0.001, 0)	1000	***1.09***	***1.07***	***1.13***	***1.11***	***1.07***	***1.10***	***1.05***	1.03	***1.05***	1.04	1.03	1.02
	500	***1.11***	***1.12***	***1.12***	***1.12***	***1.12***	***1.10***	***1.07***	***1.06***	***1.08***	***1.08***	***1.08***	***1.06***
	200	***1.13***	***1.12***	***1.14***	***1.14***	***1.13***	***1.16***	***1.11***	***1.09***	***1.10***	***1.09***	***1.11***	***1.11***
	100	***1.13***	***1.12***	***1.12***	***1.13***	***1.13***	***1.13***	***1.10***	***1.09***	***1.10***	***1.11***	***1.09***	***1.11***
	50	***1.15***	***1.12***	***1.15***	***1.15***	***1.15***	***1.15***	***1.10***	***1.09***	***1.11***	***1.11***	***1.12***	***1.11***
[-1, 0)	1000	***1.10***	***1.08***	***1.14***	***1.12***	***1.08***	***1.11***	1.00	0.989	1.01	0.997	0.987	0.976
	500	***1.15***	***1.14***	***1.15***	***1.16***	***1.14***	***1.13***	***1.05***	1.03	***1.06***	***1.05***	***1.05***	1.03
	200	***1.22***	***1.19***	***1.22***	***1.22***	***1.21***	***1.23***	***1.13***	***1.09***	***1.12***	***1.12***	***1.14***	***1.14***
	100	***1.25***	***1.23***	***1.24***	***1.25***	***1.26***	***1.25***	***1.18***	***1.13***	***1.18***	***1.19***	***1.16***	***1.18***
	50	***1.32***	***1.27***	***1.33***	***1.34***	***1.33***	***1.33***	***1.23***	***1.18***	***1.24***	***1.24***	***1.24***	***1.24***
0	1000	1.01	1.01	0.988	1.01	1.01	1.01	1.00	1.00	1.00	0.995	1.00	1.01
	500	1.01	1.01	0.997	1.02	1.01	0.997	1.01	1.00	1.01	1.02	0.999	1.00
	200	1.01	0.995	0.997	0.993	0.983	1.01	1.01	1.01	0.992	0.987	0.990	0.993
	100	1.02	0.995	1.01	1.00	0.994	1.00	1.01	0.993	0.985	0.996	0.983	0.987
	50	0.987	0.996	1.01	0.997	1.00	0.979	0.999	0.996	1.01	1.00	1.01	1.00

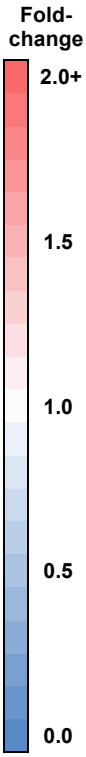

Table S6. Results from forward simulations of neutral and deleterious variation with different island population sizes. Related to Figure 4. Pictorial depictions of demographic models are shown in Figure 4A of the main text. The value in each cell represents the mean fold-change in the total number of alleles per individual in the island population relative to the mainland. For example, a value of 1.00 indicates no difference in the average number of alleles between the island and mainland, a value of 0.50 indicates that island individuals have half as many alleles relative to the mainland on average, and a value of 2.00 indicates that island individuals have twice as many alleles relative to the mainland on average. Cells are color-coded according to their value, such that blue indicates a depletion (fold-change <1.00) and red indicates an enrichment (fold-change >1.00) of the number of alleles per individual on the island relative to the mainland. The enrichment color intensity is capped at 2-fold enrichment. Values that are significant (p<0.05) are bold and italicized.

Supplemental References

S1. McLaren, W., Pritchard, B., Rios, D., Chen, Y., Flicek, P. and Cunningham, F. (2010). Deriving the consequences of genomic variants with the Ensembl API and SNP Effect Predictor. Bioinformatics 26, 2069-2070.

S2. Kumar, P., Henikoff, S. and Ng, P.C. (2009). Predicting the effects of coding non-synonymous variants on protein function using the SIFT algorithm. Nat. Protoc. 4, 1073-1081.

S3. Robinson, J.A., Ortega-Del Vecchyo, D., Fan, Z., Kim, B.Y., Marsden, C.D., Lohmueller, K.E. and Wayne, R.K. (2016). Genomic flatlining in the endangered island fox. Curr. Biol. 26, 1183-1189.